AAPS PharmSciTech, Vol. 14, No. 1, March 2013 (© 2012)
DOI: 10.1208/s12249-012-9888-y

Research Article

Design and *In Vitro* Evaluation of Finasteride-Loaded Liquid Crystalline Nanoparticles for Topical Delivery

Thiagarajan Madheswaran,[1] Rengarajan Baskaran,[1] Raj Kumar Thapa,[1] Jeong Yeon Rhyu,[1] Hye Yoon Choi,[1] Jong Oh Kim,[1] Chul Soon Yong,[1] and Bong Kyu Yoo[2,3]

Received 27 June 2012; accepted 1 November 2012; published online 4 December 2012

Abstract. In this study, liquid crystalline nanoparticles (LCN) have been proposed as new carrier for topical delivery of finasteride (FNS) in the treatment of androgenetic alopecia. To evaluate the potential of this nanocarrier, FNS-loaded LCN was prepared by ultrasonication method and characterized for size, shape, *in vitro* release, and skin permeation–retention properties. The particle size ranged from 153.8 to 170.2 nm with a cubical shape and exhibited controlled release profile with less than 20% of the drug released in the first 24 h. The release profile was significantly altered with addition of different additives. Formulation with lower monoolein exhibited higher skin permeation with a flux rate of 0.061± 0.005 $\mu g cm^{-2} h^{-1}$ in 24 h. The permeation however, significantly increased with glycerol, propylene glycol, and polyethylene glycol 400, while it declined for the addition of oleic acid. A similar trend was observed with skin retention study. In conclusion, FNS-loaded LCN could be advocated as a viable alternative for oral administration of the drug.

KEY WORDS: androgenetic alopecia; finasteride; liquid crystalline nanoparticles; release; skin permeation–retention.

INTRODUCTION

Androgenetic alopecia (AGA) is a common form of hair loss in both men and women caused by progressive miniaturization of scalp hair follicles. In AGA, scalp hair follicles exhibit increased level and activity of 5α-reductase which converts testosterone to dihydrotestosterone (DHT) (1,2). Finasteride (FNS), a synthetic 4-aza-3-oxosteroid compound with poor aqueous solubility, blocks the peripheral conversion of testosterone to DHT, resulting in a significant reduction in DHT concentration (3,4). However, oral administration of FNS may result in systemic side effects including mood disturbance, gynecomastia, decreased libido, erectile dysfunction, and ejaculation disorder (5,6). In this regard, topical route is considered a promising approach to target the drug to the site of action and minimize the unwanted side effects (7). However, the skin has evolved to be a highly effective barrier against exogenous aggressions and particles penetration.

Various nanoparticulate systems have been developed that can penetrate into the scalp skin and hair follicle openings to deliver the drug of interest (8). Liquid crystalline nanoparticles (LCN) based on monoolein (MO) have received great attention by virtue of their ability to act as nanocarriers for drugs, such as nicotine, salbutamol, acyclovir, peptides, proteins, and others (9–13). MO is a nontoxic, biodegradable, and biocompatible material (GRAS status) which can arrange itself into different ordered arrays (cubic phase and hexagonal phase) depending on water content, temperature, and presence of solutes (14). Furthermore, LCN has been previously demonstrated to enhance the permeation of drugs, such as indomethacin, and diclofenac upon topical application of the LCN (15–17). Liquid crystalline phases of MO, such as cubic phases, present interesting properties for a topical delivery system such as they (1) are bioadhesive, (2) act as a permeation enhancer (by promoting ceramide extraction and enhancement of lipid fluidity) (18), and (3) afford the ability to encapsulate compounds independent of their solubility, protecting them from physical and enzymatic degradation, and control their delivery (19–21). In particular, topical delivery of FNS was previously studied by simply incorporating it into a hydrogel base that resulted in low permeation and less therapeutic effect (22,23). In addition, topical delivery of FNS was studied by using various traditional lipid carriers. In this regard, negatively charged liposomes and niosomes of FNS were prepared and evaluated for its follicular deposition in the pilosebaceous units of hamster flank skin and ears (24). Very recently, our group demonstrated a liposomal system for the topical delivery of FNS, which however resulted only in moderate efficacy due to a limited penetration (25).

Thus, despite many investigations, none have reached the skin pharmaceutical market due to drawbacks mentioned above, necessitating a need for a system which can effectively permeate and retain the therapeutic moiety with a controlled

[1] College of Pharmacy, Yeungnam University, 214-1 Dae-dong, Gyeongsan 712-749, South Korea.
[2] College of Pharmacy, Gachon University, 191 Hambakmoero, Incheon 406-799, South Korea.
[3] To whom correspondence should be addressed. (e-mail: byoo@gachon.ac.kr)

release profile. Hence, in this work, we investigate the incorporation of FNS in LCN which is stabilized by poloxamer 407. Furthermore, with a view to understand the effect of additives on its physicochemical property and permeation parameters, we have investigated the influence of glycerol (GL), oleic acid (OA), propylene glycol (PG), and polyethylene glycol 400 (PEG). The aim was to assess the feasibility of LCN for topical delivery and more importantly to formulate a nanocarrier with enhanced permeation and retention for the potential application in AGA. To the best of our knowledge, no reports on delivery of FNS via LCN exist in the literature, to date.

MATERIALS

FNS was kindly donated from Dong-A Pharmaceutical Co., South Korea. MO was received as a gift from Danisco Japan (Tokyo, Japan). Poloxamer 407 was purchased from BASF (Ludwigshafen, Germany). Dialysis membrane was purchased from Spectrum Laboratories Inc (Rancho Dominguez, CA). All other chemicals were of analytical grade and used without further purification.

METHODS

Preparation of FNS-loaded LCN

The nanoparticles were prepared with slight modification of previously reported method (26), and the formula is given in Table I. The appropriate amount of MO was melted at 45°C, and FNS was added with vortexing for 1 min. In another glass vial, poloxamer 407 of different concentration was dissolved in water and heated at the same temperature. Poloxamer 407 solution was added to the melted MO with vortexing and equilibrated at ambient temperature for 24 h. The same method was used to prepare formulations with varied amount of MO and additives. Additives were added either to poloxamer solution or melted MO in the above mentioned method. GL was added to poloxamer solution and others (OA, PG, and PEG) were added to melted MO solution. Finally, the dispersion was subjected to sonication for 30 min using bath type sonicator (Cole-Parmer Ultrasonic 8893, Vernon Hills, IL) at 42,000 Hz.

Characterization of FNS-loaded LCN

Dynamic Light Scattering

The average hydrodynamic diameter (size) and polydispersity index (PDI) of FNS-loaded nanoparticles were assessed at 25°C by a high performance dynamic light scattering device (Zetasizer ZS, Malvern Instruments, UK) at a fixed angle of 90°. The dispersion was suitably diluted with distilled water (18.2 $M\Omega\,cm^{-1}$).

Transmission Electron Microscopy

The morphology of FNS-loaded LCN was examined using a transmission electron microscope (Hitachi 7600, Tokyo, Japan) at an accelerating voltage of 100 kV. Briefly, a drop of nanoparticle dispersion was applied on a carbon-coated copper grid and left for 1 min to allow particle adherence to substrate. A drop of 1% phosphotungstic acid solution was then applied as a negative stain followed by air-drying at room temperature.

Encapsulation Efficiency

FNS was quantified by HPLC method described elsewhere (25). Briefly, the HPLC system (Shimadzu) equipped with LC 20AD pump, SPD 20A UV–vis detector at 210 nm and SIL 20A prominence autosampler. The column used was Inertsil ODS-3 (4.6×150 mm, GL Science, Japan) and mobile phase consisted of mixture of acetonitrile and water (60:40 (*v*/*v*), pH adjusted to 2.8 with orthophosphoric acid). Ibuprofen was used as internal standard, and injection volume was 20 μl with flow rate of 1 ml/min. HPLC assay validation was performed five times a day for five consecutive days in the range of 0.05–50 μg/ml concentration. The amount of FNS encapsulated into nanoparticles was

Table I. Compositions of Various Formulations of Finasteride-Loaded Liquid Crystalline Nanoparticles and its Characterization Parameters

Formulation code	MO (%, *w*/*w*)	P 407 (%, *w*/*w*)	FNS (%, *w*/*w*)	GL (%, *w*/*w*)	OA (%, *w*/w)	PG (%, *w*/*w*)	PEG (%, *w*/w)	Particle size (nm)	PDI	Encapsulation efficiency (%)
F1	9	0.25	0.05	–	–	–	–	170.2±1.8	0.16±0.01	99.3±0.1
F2	9	0.50	0.05	–	–	–	–	153.8±3.9	0.16±0.01	99.4±0.1
F3 (MO 9)	9	1.0	0.05	–	–	–	–	160.5±3.5	0.13±0.01	99.3±0.1
F4	9	1.6	0.05	–	–	–	–	168.0±3.4	0.19±0.01	99.2±0.1
F5	9	2.2	0.05	–	–	–	–	168.4±2.9	0.18±0.01	99.3±0.1
MO 1	1.1	0.12	0.05	–	–	–	–	188.8±4.9	0.26±0.02	98.1±0.1
MO 2	2.2	0.25	0.05	–	–	–	–	176.5±7.2	0.19±0.01	98.4±0.3
MO 4.5	4.5	0.5	0.05	–	–	–	–	177.9±6.25	0.26±0.03	98.1±0.1
GL10	9	1	0.05	10	–	–	–	189.1±7.2	0.22±0.01	99.6±0.1
GL20	9	1	0.05	20	–	–	–	190.4±6.3	0.23±0.01	99.7±0.1
OA 5	9	1	0.05	–	5	–	–	220.1±4.9	0.24±0.01	99.6±0.1
OA 10	9	1	0.05	–	10	–	–	232.6±4.9	0.25±0.02	99.4±0.2
PG 10	9	1	0.05	–	–	10	–	163.1±10.4	0.23±0.02	99.8±0.1
PG 20	9	1	0.05	–	–	20	–	160.9±3.5	0.21±0.01	99.6±0.1
PEG 7.5	9	1	0.05	–	–	–	7.5	147.0±4.7	0.25±0.02	99.0±0.3
PEG 15	9	1	0.05	–	–	–	15	161.9±3.4	0.22±0.03	98.9±0.4

Each value represents the mean±SD (n=3)
MO monoolein, *P407* poloxamer 407, *FNS* finasteride, *GL* glycerol, *OA* oleic acid, *PG* propylene glycol, *PEG* polyethylene glycol 400

determined by ultrafiltration method using a specialized ultrafilter tube (Amicon Ultra-4, MWCO 10,000 g/mol, Billerica, MA). Briefly, 1 ml of nanoparticle dispersion was transferred to the upper chamber of ultrafiltration tube and centrifuged at 2,500×*g* for 15 min. Then, the filtrate containing free FNS was analyzed using HPLC. The EE was calculated from the following equation.

$$EE = \frac{D_{total} - D_{free}}{D_{total}} \times 100$$

EE Percent EE
D_{total} Amount of FNS in LCN dispersion
D_{free} Amount of FNS in the filtrate

In Vitro Drug Release Study

The *in vitro* drug release was evaluated by Franz diffusion cell using Spectra/Por® regenerated cellulose membrane of MWCO 10,000 g/mol (surface area of 2.1 cm^2). FNS dispersion equivalent to 500 μg of drug was placed in the donor compartment, and receptor compartment was filled with 10 ml of 20% (*v*/*v*) ethanol solution to maintain sink condition. FNS dissolved in 20% ethanol solution was used as control. Samples (500 μl) were withdrawn at fixed time intervals (1, 2, 3, 6, 12, and 24 h) from the receptor compartment. Samples were then analyzed by HPLC as mention above.

In Vitro Skin Permeation and Retention

Animal care and procedures were carried out according to the guidelines established for animal use in toxicology (Society of Toxicology USP 1989). The study protocol was approved by Animal Care and Use Committee, College of Pharmacy, Gachon University. A Franz diffusion cell with diffusion area of 2.1 cm^2 was used for skin permeation and retention study. Dorsal skin of 7-week-old male hairless mice was excised after killing with excess anesthesia. The adhering fat was carefully removed and washed with saline to remove extraneous debris. The skin was placed horizontally with stratum corneum facing the donor compartment. The receptor compartments were filled with 10 ml of 20% (*v*/*v*) ethanol solution, and it was maintained homogenous using stirring magnetic bar. The temperature of receptor compartment was maintained at 37°C throughout the experiment.

FNS-loaded LCN dispersion and control, equivalent to 500 μg of FNS were applied onto the skin. Serial samplings were collected at a predetermined time interval (1, 2, 3, 6, 12, and 24 h), and replaced with the same amount of fresh medium. Skin retention of FNS was determined at the end of permeation study. Briefly, skin was minced (with surgical scalpel) and added to a glass vial containing 5 ml of ethanol water mixture (3:2, *v*/*v*) and homogenized (Ultra-Turrax T25 Basic, Germany) for 10 min under ice bath. The supernatant was centrifuged (Eppendorf 5415 D) at 12,000×*g* for 5 min. Then, the upper layer was mixed with same volume of absolute ethanol and vortexed for 30 s, followed by centrifugation at 16,000×*g*. The filtrate was analyzed by HPLC as mentioned above.

Statistical Analysis

All the data obtained were analyzed by Student's *t* test using SPSS software (version 10). Data are presented as mean±standard deviation. A value of $p<0.05$ was considered statistically significant.

RESULTS

Hydrodynamic Size and PDI

The average particle size of all the formulations without additives were in the range of 153.8–170.2 nm with narrow size distribution (PDI≤0.26). There was no significant difference in the particle size between formulations prepared with various concentration of poloxamer 407 (F1–F5). Additives impact on the particle size was investigated. All the additives showed negligible or insignificant influence on size with the exception of OA. OA addition caused significant increase in the size of the LCN (>220 nm).

The PDI values were lower than 0.3, suggesting narrow size distribution and suitability of preparation method employed in this study. While PDI increased with the addition of additives, it remained in the range which indicates monodispersed dispersion. Typical particle size distribution of FNS-loaded LCN is shown in Fig. 1a.

Morphological Imaging

Transmission electron microscopy (TEM) revealed discrete and monodispersed nanoparticles in consistent with the dynamic light scattering characterization. The nanoparticle appears like cubical structure which indicates the formation of cubic phases of liquid crystalline system. TEM image clearly shows that the particles possess multiple black dots, which represent phosphotungstic acid-stained water channels. Furthermore, drug incorporation did not influence the size of the nanoparticles and the particles are well separated with no apparent signs of aggregation (Fig. 1b, c).

Encapsulation Efficiency

EE of all the formulations were more than 98% (Table I). This implies that most of the drug was encapsulated in the LCN. Although particle size was significantly increased when OA was added, there was no significant influence on EE probably because of extremely high encapsulation of the drug.

In Vitro Drug Release Study

Figure 2a illustrates the difference in release rate of FNS from formulations with varying surfactant concentrations. The release was found to be similar at all the concentrations of surfactant. The nanoparticles showed a controlled release profile for FNS comparing to control which released more than 80% of the drug within 24 h of the study period. In contrast to surfactant, slow drug release was observed with

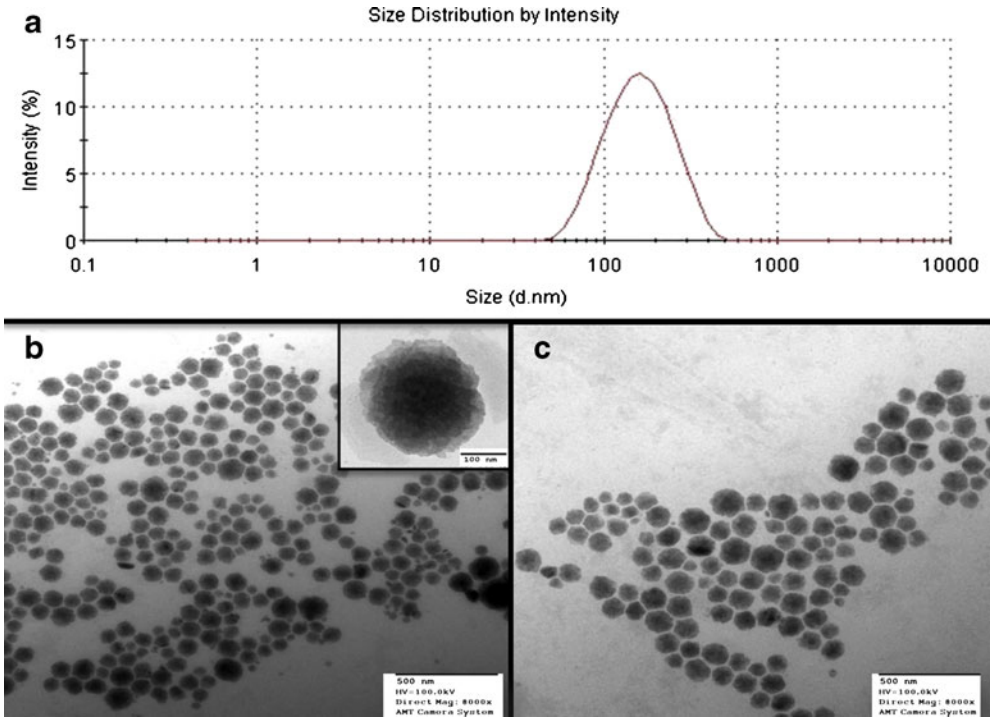

Fig. 1. **a** Typical particle size distribution of FNS-loaded LCN. **b** TEM image of blank nanoparticles (*inset*, high-magnification image of single nanoparticle). **c** TEM image of FNS-loaded LCN

increase in the MO amount (Fig. 2b). The release of FNS increased with the addition of 10% and 20% of GL in comparison to formulation MO 9 (Fig. 2c). Similarly, the FNS release increased with the addition of PG and PEG (Fig. 2e, f). However, the release decreased significantly with the addition of 5% and 10% OA, (Fig. 2d, $p<0.05$). Kinetic parameters for drug release from the LCN are summarized in Table II.

In Vitro Skin Permeation and Retention

In the present study, skin permeation was carried out with Franz diffusion cell using excised male mice skin. Overall, the skin permeation of FNS-loaded LCN was high compared with control. Permeation parameters and percentage of drug at the end of the permeation study are summarized in Table III. FNS permeation declined with the further increase in the amount of MO. In line with this findings, Q_{cum} and J_{flux} were significantly less for MO 9 (prepared with highest MO concentration), compared with MO 1 and MO 2 prepared with lower MO concentration ($p<0.01$). The permeation of formulations prepared with additives was compared with MO 9. As anticipated, GL, PG, and PEG increased the drug permeation while OA decreased cumulative permeation of drug. The drug permeation through the skin followed zero-order kinetics with controlled release (Table III).

DISCUSSION

Despite the market abundance of commercially available dermo-cosmetic agent claiming miraculous elimination of AGA, overwhelming limitations continue to exit till this date (27). In this regard, oral FNS is indicated for the treatment of AGA. However, since oral administration of FNS may result in systemic side effects, it was hypothesized that topical delivery of FNS might be effective in treating AGA. Hence, we aimed to formulate a system that would provide topical delivery of FNS while eliminating potential drawbacks. In order to maintain high skin retention in scalp and enable lower dosing frequency, we prepared FNS-loaded LCN as new controlled delivery systems.

Herein, we have successfully prepared FNS-loaded LCN by the ultrasonication method via optimizing several key process and formulation variables. In this study, poloxamer 407 was used in the weight percentage of 2.5–20% (*w*/*w*; F1-F5) with respect to MO. Aforementioned surfactant ranges were selected based on the previous research in this area which suggests a formation of stable nanoparticles (28,29). Among the various formulations, there was no significant difference in the particle size which is consistent with our previous observation (30). This could be because poloxamer 407 covered the whole nanoparticle surface at the lowest concentration. Additionally, poloxamer 407 has been shown not to affect the internal structure of the system. This might be explained by the fact that poloxamer 407 being a large molecule is excluded from the water channels while the cubic structure was forming (28,31).

TEM is a useful tool to examine the morphology and nanostructural characteristic of the dispersed nanoparticles. The appearance of numerous black dots in the particles confirms the formation of liquid crystalline phase (32,33). The high EE of FNS in the LCN could be due to the high lipophilic properties of MO and FNS that tends to encapsulate the drug in the lipid bi-layer of nanoparticles.

Many parameters influence the drug release from nanoparticles. Among all, surfactant plays a pivotal role in the stability of nanoparticles and hence the release as it gets anchored at the interface of lipid bi-layer and aqueous phase

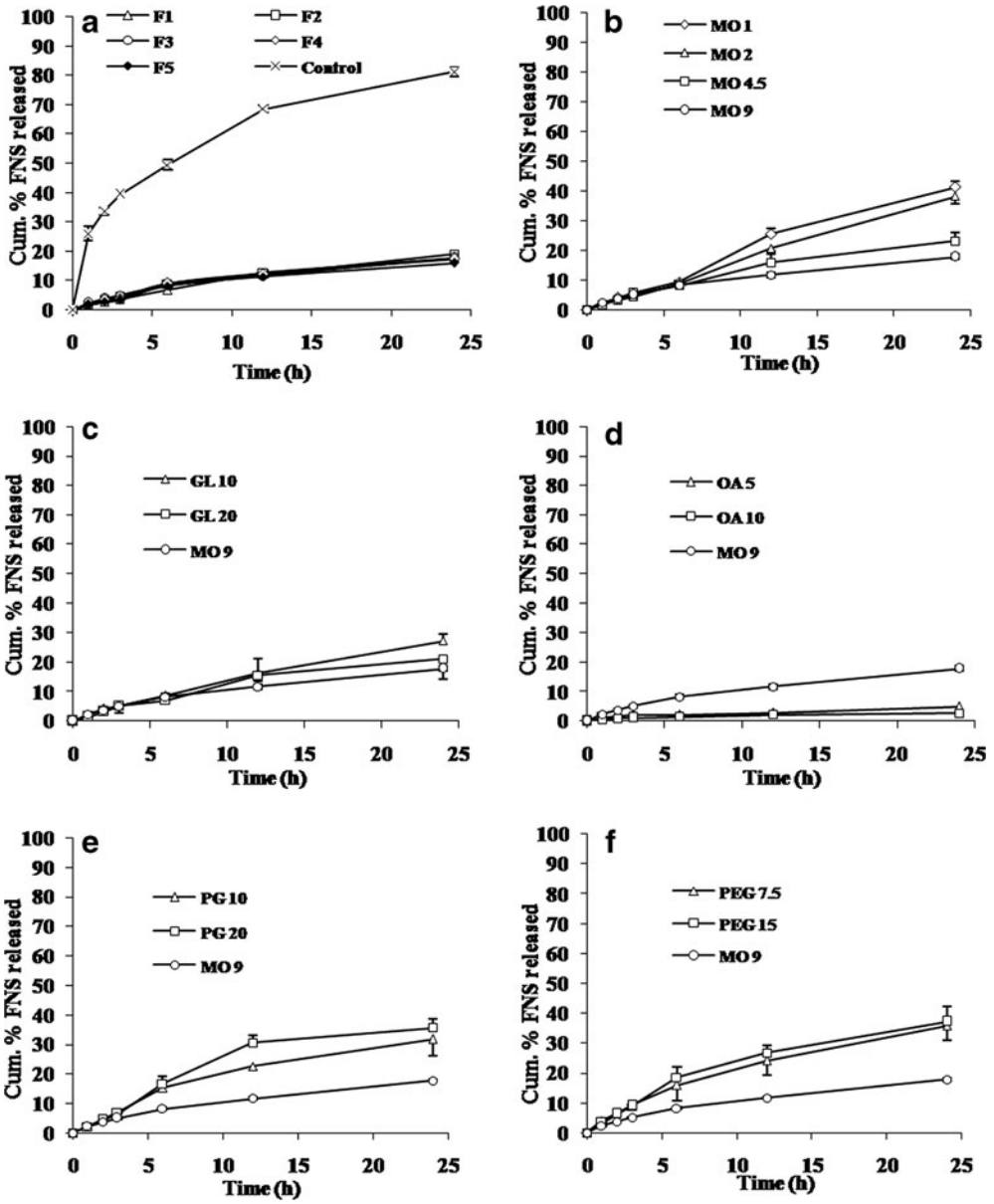

Fig. 2. Cumulative release profile of FNS from LCN. Each value represents mean±SD (n=3). **a** Effect of poloxamer 407. **b** Effect of MO. **c** Effect of GL. **d** Effect of OA. **e** Effect of PG. **f** Effect of PEG

(28,29,31). However, there was no significant difference in the present study. This implies that the surfactant covers the whole nanoparticle surface even at the lowest concentration (34). Thus, a further increase in the surfactant level did not have any influence on the release profile. However, the release was slowed down in proportion to the amount of MO. The delayed release appears to be attributed to slow diffusion of FNS from lipid bi-layer which strongly holds the drug within hydrophobic domain of the bi-layer.

In the present study, the release of drug from the liquid crystalline matrices formed with GL, OA, PG, and PEG were assessed. Increase in the release was observed with addition of GL, PG, and PEG. The increased release may be attributed to less hydrophobic microenvironment inside the nanoparticles caused by the additives, which favors the quick escape of drug from the lipid bi-layer to aqueous phase. PG and PEG partition well into the lipid and aqueous interfacial domains and affect the internal curvature of liquid crystalline phase by allowing to swell the aqueous pore, and hence faster release of drug (35,36). The decrease in the release with addition of OA may be due to increase in the hydrophobicity of the formulation owing to an increase in the apparent hydrophobic volume of lipid transforming the mesophase (37). Electrostatic interaction due to the presence of OA may also affect the curvature of lipid bi-layer and eventually change the average surface area of lipid head group. This leads to a change in monoglyceride molecular packing and causes a transition from cubic to hexagonal phase (38,39).

To describe the kinetics of drug release from LCN dispersion, mathematical modeling has been proposed. Briefly, zero-order describes a system where drug release is independent of its concentration, while a first-order model describes a concentration-dependent one. In the Higuchi model, drug release from an insoluble matrix is directly proportional to

Table II. Kinetic Parameters for *in vitro* Drug Release and Skin Permeation of the Finasteride-Loaded Liquid Crystalline Nanoparticles

Formulation code	*In vitro* drug release					*In vitro* skin permeation			
	Zero-order kinetics (r^2)	First-order kinetics (r^2)	Higuchi kinetics (r^2)	Korsmeyer–Peppas kinetics		Zero-order kinetics (r^2)	Higuchi kinetics (r^2)	Korsmeyer–Peppas kinetics	
				r^2	n			r^2	n
F1	0.960	0.968	0.992	0.994	0.80	nd	nd	nd	nd
F2	0.959	0.969	0.992	0.981	0.74	nd	nd	nd	nd
F3 (MO 9)	0.968	0.976	0.998	0.996	0.64	0.987	0.813	0.987	1.27
F4	0.928	0.939	0.985	0.977	0.72	nd	nd	nd	nd
F5	0.926	0.936	0.983	0.976	0.75	nd	nd	nd	nd
MO 1	0.968	0.977	0.993	0.987	0.83	0.984	0.835	0.853	1.19
MO 2	0.885	0.901	0.996	0.982	0.67	0.980	0.830	0.884	1.37
MO 4.5	0.958	0.935	0.998	0.996	0.99	0.985	0.843	0.680	1.33
GL 10	0.953	0.967	0.986	0.998	0.78	0.935	0.843	0.797	1.16
GL 20	0.947	0.957	0.981	0.976	0.83	0.935	0.843	0.792	1.15
OA 5	0.951	0.953	0.997	0.922	0.46	0.992	0.876	0.845	0.84
OA 10	0.862	0.864	0.983	0.952	0.55	0	0.883	0.810	0.99
PG 10	0.933	0.955	0.990	0.976	0.84	0.996	0.892	0.876	1.19
PG 20	0.873	0.895	0.993	0.966	0.95	0.969	0.806	0.880	1.25
PEG 7.5	0.966	0.959	0.999	0.996	0.69	0.986	0.842	0.882	1.30
PEG 15	0.961	0.982	0.998	0.979	0.79	0.979	0.865	0.831	1.44

Each value represents the mean (n=3)
nd not determined, r^2 correlation coefficient of linear regression, *MO* monoolein, *P407* poloxamer 407, *GL* glycerol, *OA* oleic acid, *PG* propylene glycol, *PEG* polyethylene glycol 400

the square root of time (10). Release data were fitted to various mathematical models such as zero order, first order, Higuchi, and Korsmeyer–Peppas to examine the path and mechanism of drug release. All formulations seem to follow a Higuchi model for the drug release based on the higher r^2 values (r^2>0.976) compared with the other three kinetic models examined (Table II). Therefore, it appears that *in-vitro* release of FNS from the LCN dispersion is primarily governed by diffusion-based mechanism, where the release decreased with time owing to an increase in the diffusional path length. However, *in vitro* skin permeation study revealed zero order kinetics probably due to complex structure of the skin compared to the cellulose membrane used in release study.

Formulations with varied amount of MO showed increase in the permeation of drug compared with control due to the better penetrability of MO through the skin (40). In this study, the additives were considered as useful strategic approach in developing topical delivery. Additives were selected to study

Table III. Mean Cumulative Permeation of Finasteride from Various Formulations Via Excised Mice Skin and Mean Percentage of FNS at the End of Study

Formulation code	Permeation parameters					Percentage of FNS at the end of permeation study		
	Q_{cum} ($\mu g cm^{-2}$)	Flux ($\mu g cm^{-2} h^{-1}$)	T_L (h)	ER	Skin retention ($\mu g cm^{-2}$)	Receptor	Donor	Skin deposition
MO 1	21.3±1.6***, *****	0.048±0.003***, *****	3.72±0.23	2.59	107.8±3.5***, ******	8.9±0.6	27.7±1.1	45.2±2.6
MO 2	27.3±2.1**, *****	0.061±0.005***, *****	2.74±0.23	3.32	83.6±1.6***, ******	11.9±0.9	34.8±2.7	35.1±0.7
MO 4.5	17.6±0.6**	0.040±0.001**, ****	2.92±0.16	2.14	33.3±1.7*, ****	7.4±0.3	61.8±3.8	13.9±0.6
MO 9	15.1±0.5**	0.034±0.002**	2.58±0.04	1.84	26.5±6.3	6.4±0.2	64.2±6.8	11.2±1.4
GL 10	22.8±3.5***, ****	0.052±0.008**, ****	4.33±0.53	2.78	37.0±2.1*, ****	9.6±1.5	69.5±1.2	15.5±0.9
GL 20	25.0±4.2****	0.056±0.009**, ****	4.19±0.35	3.04	31.2±2.4*	10.5±1.8	64.8±4.1	13.1±1.0
OA 5	9.4±3.0	0.018±0.007	0.82±1.77	1.14	27.4±0.9	3.9±1.3	74.1±6.3	11.5±0.4
OA 10	8.6±0.7	0.018±0.001	1.35±0.35	1.04	25.7±1.0	3.7±0.3	79.4±6.5	10.7±0.4
PG 10	20.2±3.2**	0.040±0.004**, ****	0.46±1.91	2.48	58.6±11.9**, ****	8.5±1.3	58.2±8.2	24.6±4.9
PG 20	22.1±3.8**, ****	0.048±0.007**, ****	3.06±0.46	2.69	60.9±4.5***, ******	9.3±1.6	55.3±7.7	25.6±1.9
PEG 7.5	22.5±7.5*	0.050±0.016*	2.61±0.69	2.74	74.0±2.6***, ******	9.5±3.1	53.9±3.8	31.1±1.0
PEG 15	30.4±5.3**, *****	0.067±0.001**, *****	1.65±1.10	3.70	76.6±11.1**, *****	12.8±2.2	50.1±3.4	32.2±4.6
Control	8.2±0.2	0.017±0.001	1.70±0.12	–	21.1±5.6	3.5±0.1	81.4±1.9	8.8±2.3

Each value represents the mean±SD (n=3)
MO monoolein, *P407* poloxamer 407, *GL* glycerol, *OA* oleic acid, *PG* propylene glycol, *PEG* polyethylene glycol 400, Q_{cum} cumulative amount of FNS permeated in 24 h, T_L lag time, *ER* enhancement ratio of Q_{cum} compared with control (FNS dissolved in 20% ethanol solution)
*p<0.05; **p<0.01; ***p<0.001—compared with control; ****p<0.05; *****p<0.01; ******p<0.001—compared with MO 9

its influence on cumulative release, skin permeation, and retention. The addition of GL, PG, and PEG increased the permeation of FNS which is consistent with the other researcher's findings. For example, cyclosporin A dissolved in formulations containing higher proportions of PG resulted in increased topical delivery (41–43). Kwon and Kim demonstrated a higher flux for minoxidil when MO was formulated with PG (33). This was attributed to the fact that PG permeates into skin and helps the skin absorb the drug. In addition, PG also exhibited the co-solvent effect which could increase thermodynamic activity of drug in the vehicle due to its volatile property. Despite the fact that OA is a powerful penetration enhancer, it resulted in lower permeability. This is probably because much of the OA incorporated was retained within the lipophilic area of LCN, resulting in poor permeability enhancing effect (44).

Consistent with skin permeation study, skin retention of FNS increased significantly with lower MO content and with incorporation of additives (40,42). One of the reasons why the skin retention of drug was high when FNS-loaded LCN was co-formulated with additives may be that these could act as co-solvents for FNS absorption within the skin (44).

CONCLUSIONS

Present study demonstrates that drug release, permeation, and retention of FNS-loaded LCN were controllable by the amount of MO and additives. The encouraging results obtained from this study advocate that liquid crystalline system could be proposed as a viable alternative for the oral administration of FNS. This finding may open new door to formulate LCN for potential applications in dermo-cosmetic and pharmaceutical fields.

ACKNOWLEDGMENTS

This work was funded by BK 21 offered by Korean Government.

REFERENCES

1. Bingham KD, Shaw DA. The metabolism of testosterone by human male scalp skin. J Endocrinol. 1973;57:111–21.
2. Schweikert HU, Wilson JD. Regulation of human hair growth by steroid hormones. I. Testosterone metabolism in isolated hairs. J Clin Endocrinol Metab. 1974;38:811–9.
3. Rathnayake D, Sinclair R. Male androgenetic alopecia. Expert Opin Pharmacother. 2010;11:1295–304.
4. Finn DA, Beadles-Bohling AS, Beckley EH, Ford MM, Gililland KR, Gorin-Meyer RE, Wiren KM. A new look at the 5α-reductase inhibitor finasteride. CNS Drug Rev. 2006;12:53–76.
5. Irwig MS, Kolukula S. Persistent sexual side effects of finasteride for male pattern hair loss. J Sex Med. 2011;8:1747–53.
6. Chaudhary UB, Turner JS. Finasteride. Expert Opin Drug Metab Toxicol. 2010;6:873–81.
7. Kogan A, Garti N. Microemulsions as transdermal drug delivery vehicles. Adv Colloid Interface Sci. 2006;123–126:369–85.
8. Padois K, Cantiéni C, Bertholle V, Bardel C, Pirot F, Falson F. Solid lipid nanoparticles suspension *versus* commercial solutions for dermal delivery of minoxidil. Int J Pharm. 2011;416:300–4.
9. Carr MG, Corish J, Corrigan OI. Drug delivery from a liquid crystalline base across Visking and human stratum corneum. Int J Pharm. 1997;157:35–42.
10. Helledi LS, Schubert L. Release kinetics of acyclovir from a suspension of acyclovir incorporated in a cubic phase delivery system. Drug Dev Ind Pharm. 2001;27:1073–81.
11. Bender J, Ericson MB, Merclin N, Iani V, Rosén A, Engström S, Moan J. Lipid cubic phases for improved topical drug delivery in photodynamic therapy. J Control Release. 2005;106:350–60.
12. Popescu G, Baraukas J, Nylander T, Tiberg F. Liquid crystalline phase and their dispersions in aqueous mixtures of glyceryl monooleate and glyceryl monoethyl ether. Langmuir. 2007;23:496–503.
13. Fraser S, Separovic F, Polyzos A. Cubic phases of ternary amphiphile-water systems. Eur Biophys J. 2009;39:83–90.
14. Larsson K. Cubic lipid-water phases: structures and biomembrane aspects. J Phys Chem. 1989;93:7304–14.
15. Esposito E, Cortesi R, Drechsler M, Paccamiccio L, Mariani P, Contado C, Stellin E, Menegatti E, Bonina F, Puglia C. Cubosome dispersions as delivery systems for percutaneous administration of indomethacin. Pharm Res. 2005;22:2163–73.
16. Turchiello RF, Vena FC, Maillard P, Souza CS, Bentley MV, Tedesco AC. Cubic phase gel as a drug delivery system for topical application of 5-ALA, its ester derivatives and m-THPC in photodynamic therapy (PDT). J Photochem Photobiol B. 2003;70:1–6.
17. Yariv D, Efrat R, Libster D, Aserin A, Garti N. *In vitro* permeation of diclofenac salts from lyotropic liquid crystalline systems. Colloids Surf B Biointerfaces. 2010;78:185–92.
18. Ogiso T, Iwaki M, Paku T. Effect of various enhancers on transdermal penetration of indomethacin and urea and relationship between penetration parameters and enhancement factors. J Pharm Sci. 1995;84:482–8.
19. Drummond CJ, Fong C. Surfactant self-assembly objects as novel drug delivery vehicles. Curr Opin Colloid Interface Sci. 1999;4:449–56.
20. Boyd BJ, Whittaker DV, Khoo S, Davey G. Lyotropic liquid crystalline phases formed from glycerate surfactants as sustained release drug delivery systems. Int J Pharm. 2006;309:218–26.
21. Gan L, Han S, Shen J, Zhu J, Zhu C, Zhang X, Gan Y. Self-assembled liquid crystalline nanoparticles as a novel ophthalmic delivery system for dexamethasone: improving preocular retention and ocular bioavailability. Int J Pharm. 2010;396:179–87.
22. Sintov A, Serafimovich S, Gilhar A. New topical antiandrogenic formulations can stimulate hair growth in human bald scalp grafted onto mice. Int J Pharm. 2000;194:125–34.
23. Hajheydari Z, Akbari J, Saeedi M, Shokoohi L. Comparing the therapeutic effects of finasteride gel and tablet in treatment of the androgenetic alopecia. Indian J Dermatol Venereol Leprol. 2009;75:47–51.
24. Tabbakhian M, Tavakoli N, Jaafari M, Daneshamouz S. Enhancement of follicular delivery of finasteride by liposomes and niosomes 1. *In vitro* permeation and *in vivo* deposition studies using hamster flank and ear models. Int J Pharm. 2006;323:1–10.
25. Lee SI, Nagayya-Sriraman S, Shanmugam S, Baskaran R, Yong CS, Yoon SK, Choi HG, Yoo BK. Effect of charge carrier on skin penetration, retention, and hair growth of topically applied finasteride-containing liposomes. Biomol Ther. 2011;19:231–6.
26. Dong YD, Larson I, Hanley T, Boyd BJ. Bulk and dispersed aqueous phase behavior of phytantriol: effect of vitamin E acetate and F127 polymer on liquid crystal nanostructure. Langmuir. 2006;22:9512–8.
27. Price VH. Treatment of hair loss. N Engl J Med. 1999;341:964–73.
28. Gustafsson J, Ljusberg-Wahren H, Almgren M, Larsson K. Submicron particles of reversed lipid phases in water stabilized by a nonionic amphiphilic polymer. Langmuir. 1997;13:6964–71.
29. Spicer PT, Hayden KL. Novel process for producing cubic liquid crystalline nanoparticles (cubosomes). Langmuir. 2001;17:5748–56.
30. Thapa R, Baskaran R, Madheswaran T, Kim JO, Yong CS, Yoo BK. Preparation, characterization, and release study of tacrolimus-loaded liquid crystalline nanoparticles. J Disp Sci Technol. 2011. doi:10.1080/01932691.2011.648462.
31. Guo C, Wang J, Cao F, Lee RJ, Zhai G. Lyotropic liquid crystal systems in drug delivery. Drug Discov Today. 2010;15:1032–40.
32. Spicer PT. Progress in liquid crystalline dispersions: cubosomes. Curr Opin Colloid Interface Sci. 2005;10:274–9.
33. Kwon TK, Kim JC. *In vitro* skin permeation of monoolein nanoparticles containing hydroxypropyl β-cyclodextrin/minoxidil complex. Int J Pharm. 2010;392:268–73.

34. Schubert MA, Müller-Goymann CC. Characterization of surface-modified solid lipid nanoparticles (SLN): influence of lecithin and nonionic emulsifier. Eur J Pharm Biopharm. 2005;61:77–86.
35. Alfons K, Engstrom S. Drug compatability with the sponge phases formed in monoolein, water, and propylene glycol or poly(ethylene glycol). J Pharm Sci. 1998;87:1527–30.
36. Angelova A, Angelov B, Mutafchieva R, Garamus VM, Lesieur S, Funari SS, Willumeit R, Couvreur P. Swelling of a sponge lipid phase via incorporation of a nonionic amphiphile: SANS and SAXS studies. Prog Colloid Polym Sci. 2011;138:1–6.
37. Chang CM, Bodmeier R. Effect of dissolution media and additives on the drug release from cubic phase delivery systems. J Control Release. 1997;46:215–22.
38. Caboi F, Nylander T, Razumas V, Talaikyté Z, Monduzzi M, Larsson K. Structural effects, mobility, and redox behavior of vitamin K1 hosted in the monoolein/water liquid crystalline phases. Langmuir. 1997;13:5476–83.
39. Lara MG, Bentley MV, Collett JH. *In vitro* drug release mechanism and drug loading studies of cubic phase gels. Int J Pharm. 2005;293:241–50.
40. Lopes LB, Lopes JL, Oliveria CR, Thomazini JA, Garcia MT, Fantini MC, Collett JH, Bentley MV. Liquid crystalline phase of monoolein and water for topical delivery of cyclosporin A: characterization and study of *in vitro* and *in vivo* delivery. Eur J Pharm Biopharm. 2006;63:146–55.
41. Lopes LB, Ferreira DA, Paula DD, Garcia MT, Thomazini JA, Fantini MC, Bentley MV. Reverse hexagonal phase nanodispersion of peptide of monoolein and oleic acid for topical delivery of peptides: *in vitro* and *in vivo* penetration of cyclosporin A. Pharm Res. 2006;23:1332–42.
42. Lopes LB, Collett JH, Bentley MV. Topical delivery of cyclosporin A: an *in vitro* study using monoolein as a penetration enhancer. Eur J Pharm Biopharm. 2005;60:25–30.
43. Herai H, Gratieri T, Thomazine JA, Bentley MV, Lopez RFV. Doxorubicin skin penetration from monoolein-containing propylene glycol formulations. Int J Pharm. 2007;329:88–93.
44. Han IH, Choi SU, Nam DY, Park YM, Kang MJ, Kang KH, Kim YM, Bae G, Oh IY, Park JH, Ye JS, Choi YB, Kim DK, Lee J, Choi YW. Identification and assessment of permeability enhancing vehicles for transdermal delivery of glucosamine hydrochloride. Arch Pharm Res. 2010;33:293–9.